Springer

Journal of
Mechanical
Science and
Technology

Journal of Mechanical Science and Technology 22 (2008) 545~555

www.springerlink.com/content/1738-494x

Experimental investigation on the airside performance of fin-and-tube heat exchangers having herringbone wave fins and proposal of a new heat transfer and pressure drop correlation

Nae-Hyun Kim[1,*], Jung-Ho Ham[2] and Jin-Pyo Cho[2]

[1]*Department of Mechanical Engineering, University of Incheon 177 Dohwa-Dong, Nam-Gu, Incheon, 402-749, Korea*
[2]*Graduate School, University of Incheon 177 Dohwa-Dong, Nam-Gu, Incheon, 402-749, Korea*

(Manuscript Received June 5, 2007; Revised October 17, 2007; Accepted November 28, 2007)

Abstract

The heat transfer and friction characteristics of fin-and-tube heat exchangers having herringbone wave fins were experimentally investigated. Eighteen samples having different fin pitches (1.34 mm to 2.54 mm) and tube rows (one to four) were tested. For all the samples, the waffle depth and the corrugation angle of the fin was 1.14 mm and 11.7° respectively. Results showed that the j factors were insensitive to fin pitch, while f factors increased as the fin pitch increased. As the number of tube rows increased, both the j and f factors decreased. However, the effect of tube row diminished as the Reynolds number increased, at least for j factors. Existing correlations failed to adequately predict the present data. A new correlation was developed based on existing data, which significantly improved the predictions of the present data.

Keywords: Heat exchanger; Heat transfer coefficient; Pressure drop; Fin-and-tube; Herringbone wave

1. Introduction

Fin-and-tube tube heat exchangers have been used for heat exchange between gases and liquids for many years. In a forced convective heat transfer between gas and liquid, the controlling thermal resistance is on the gas-side, and specially configured fins have been used to improve the gas-side performance. Webb and Kim [1] and Wang [2] provide recent progress on this issue. Of the many enhanced geometries, wave fins have long been used in air-conditioning or process industries. Wave fins provide considerable heat transfer enhancement with manageable pressure drop. For a wave fin, the enhancement is known to be achieved by the action of streamwise (Goertler) and spanwise vortices [3, 4], which provide better mixing of the flow. There are two basic variants of the wave fin

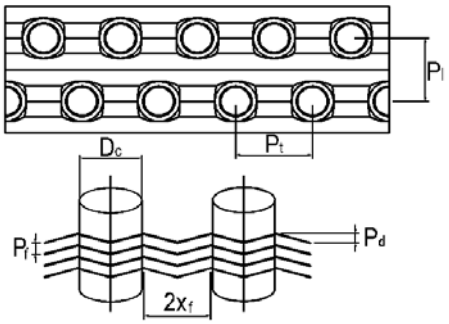

(a) Herringbon wave

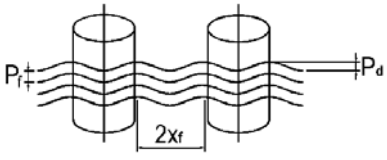

(b) Smooth wave

Fig. 1. Schematic drawing of typical herringbone wave and smooth wave fin-and-tube heat exchangers.

*Corresponding author. Tel.: +82 32 770 8421, Fax.: +82 32 770 8410
E-mail address: knh0001@lncheon.ac.kr
DOI 10.1007/s12206-007-1116-4

geometry [5]. They may have a smooth wave configuration, or they may have a herringbone configuration, as illustrated in Fig. 1.

Although wave fins are widely used in industry, the heat transfer or friction data are very limited. Existing experimental investigations are summarized in Table 1. Goldstein and Sparrow [3] measured the local and average mass transfer coefficient for the herringbone wave fin configuration using a mass transfer technique. They reported that the herringbone wave provided 45% higher mass transfer coefficient than the plain fin at Re_{Dc} = 1000. Their test simulated one row geometry having 606 fins per meter on an 8.53 mm diameter tube. Beecher and Fagan [6] published heat transfer data for 21 herringbone wave geometries having a three-row configuration. Their models consisted of a pair of brass plates and spacers to simulate a fin-and-tube geometry. The channel walls were electrically heated, and thermocouples were embedded in the plates to determine the plate surface temperatures.

Recently, Wang and co-workers [7-10] provided extensive test results for herringbone wave fin heat exchangers. Wang et al. [7] tested eighteen heat exchangers, which had P_d=1.5 mm, D_c=10.3 mm, P_t=25.4mm, P_l=19.05 mm, 1.69 mm ≤ P_f ≤ 3.53 mm, 1 ≤ N ≤ 4. The friction factors were almost independent of the number of tube rows, and increased as the fin pitch increased. On the contrary, the j factors decreased as the number of tube row increased, and were almost independent of the fin pitch. Similar conclusions were drawn from Wang et al. [8], who tested seven herringbone wave fin heat exchangers that had smaller waffle height and tube diameter (P_d=1.32 mm, D_c=8.64 mm, P_t=25.4 mm, P_l=19.05 mm, 1.21 mm ≤ P_f ≤ 2.54 mm, 1 ≤ N ≤ 4). For a large tube diameter and fin pitch (D_c=16.88 mm, 2.98 mm ≤ P_f ≤ 6.45 mm, P_d=1.8 mm, P_t=38.1 mm, P_l=33.0 mm, 1 ≤ N ≤ 6), however, Wang et al. [9] reported that both the j factors and friction factors increased as the fin pitch increased. The effects of the number of tube rows were the same as those of the previous investigations [7, 8]. To investigate the effect of waffle height on the friction and j factors, Wang et al. [10] tested twelve heat exchangers having two different waffle heights (P_d=1.18 mm and 1.58 mm, 1.65 mm ≤ P_f ≤ 3.17 mm, D_c =8.62 mm, P_t=25.4 mm, P_l=19.05 mm, N = 2, 4). For a shallow waffle depth (P_d = 1.18 mm), the effects of fin pitch or the number of tube rows on the friction or j factors were the same as those of the previous investigations [7, 8]. The friction factors were almost independent of the number of tube rows, and increased as the fin pitch increased. The j factors decreased as the number of tube rows increased, and were almost independent of the fin pitch. For a deep waffle depth (P_d=1.58 mm),

Table 1. Previous experimental investigations on the thermal performance of heat exchangers having wave fins.

Investigator	Wave pattern	D_c (mm)	P_f (mm)	P_t (mm)	P_l (mm)	N	x_f (mm)	P_d (mm)	α (deg)
Goldstein & Sparrow(1976)	H*	8.53	1.65	21.3	N/A	1	4.63	1.78	21.0
Beecher & Fagan(1987)	H	7.94-12.7	2.08-7.97	25.4-31.8	22.0-27.5	3	2.76-5.50	0.97-3.18	10.0-34.7
Wang et al. (1997)	H	10.3	3.53	25.4	19.05	1,2,3,4	4.76	1.5	17.5
Wang et al. (1998)	H	8.54	1.21-2.54	25.4	19.05	1,2,4	4.76	1.32	15.5
Wang et al. (1999a)	H	13.6-16.9	3.04-6.45	31.8-38.1	27.5, 33	1,2,4,6	6.88, 8.25	1.8	12.3. 14.7
Wang et al. (1999b)	H	8.62	1.68-3.17	25.4	19.05	2,4	4.76	1.18-1.58	14.9-18.4
Saiz Jabardo et al. (2006)	H	12.7	1.81~3.17	31.75	27.5	1,2,3,4	5.5	1.83	18.4
Mirth & Ramdhyani (1994)	S	13.2, 16.4	3.12-6.15	31.8, 38.1		4,8	6.875	2.38, 3.25	19.1-25.3
Kim et al. (2004)	S	10.3	1.3-1.7	25.4	21.65	1,2,3	5.41	1.5. 2.0	15.5, 20.3
Present study	H	10.03	1.34~2.54	25.4	22.0	1,2,3,4	5.5	1.14	11.7

* 'H' denotes 'herringbone' and 'S' denotes 'smooth'

however, the j factors decreased as the fin pitch increased. Similar conclusion was drawn from Saiz Jabardo et al. [11], who tested seven herringbone wave heat exchangers having a deep waffle depth (P_d=1.83 mm, D_c=12.7 mm, 1.81 mm ≤ P_f ≤ 3.17 mm, P_t=31.75 mm, P_l=27.5 mm, 1 ≤ N ≤ 4). The j factors decreased as the fin pitch increased. Additional investigations on the friction and j factors of the herringbone wave heat exchangers include Wongwises and Chokeman [12] and Chokeman and Wongwises [13], who investigated the effect of fin thickness and the effect of fin collar pattern, respectively. Compared to the herringbone wave configuration, little information is available for the smooth wave fin configuration. Mirth and Ramadhyani [14] tested five cores having two different fin patterns with four or eight rows. Kim et al. [15] reported test data for eighteen samples having two different waffle heights (P_d = 1.5mm and 2.0 mm).

The available data range of the herringbone wave heat exchangers is plotted in Fig. 2 as a function of P_d and D_c. Fig. 2 reveals that more data are needed, especially for small waffle heights. In the present study, eighteen herringbone wave heat exchangers having P_d = 1.14 mm (D_c = 10.03 mm, 1.34 ≤ P_f ≤ 2.54 mm, P_t = 25.2 mm, P_l = 22.0 mm, 1 ≤ N ≤ 4) were tested. As shown in Fig. 2, the present data contribute to extend the database. As shown in Table 1, the corrugation angle of the present wave fin (11.7°) is the lowest ever tested. The present wavy fin configuration has many applications including coils for air handling units, industrial condensers, etc.

2. Experiments

2.1 Heat exchanger samples

A total of eighteen heat exchangers were tested in the present study. The height and the width of the samples were 250 mm and 400 mm, respectively. The geometric parameters are listed in Table 2, and detailed

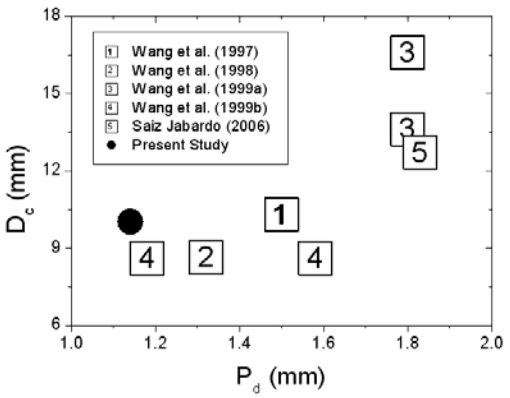

Fig. 2. Existing data range on the thermal performance of herringbone wave fin-and-tube heat exchangers.

Table 2. Geometric dimensions of the sample heat exchangers.

No	Fin Shape	P_f(mm)	N	P_d(mm)	x_f(mm)	D_c(mm)	P_t(mm)	P_l(mm)
1	herringbone wave	1.34	1	1.14	5.5	10.03	25.4	22.0
2	herringbone wave	1.49	1	1.14	5.5	10.03	25.4	22.0
3	herringbone wave	1.69	1	1.14	5.5	10.03	25.4	22.0
4	herringbone wave	1.81	1	1.14	5.5	10.03	25.4	22.0
5	herringbone wave	2.12	1	1.14	5.5	10.03	25.4	22.0
6	herringbone wave	2.54	1	1.14	5.5	10.03	25.4	22.0
7	herringbone wave	1.34	2	1.14	5.5	10.03	25.4	22.0
8	herringbone wave	1.49	2	1.14	5.5	10.03	25.4	22.0
9	herringbone wave	1.69	2	1.14	5.5	10.03	25.4	22.0
10	herringbone wave	1.81	2	1.14	5.5	10.03	25.4	22.0
11	herringbone wave	2.12	2	1.14	5.5	10.03	25.4	22.0
12	herringbone wave	2.54	2	1.14	5.5	10.03	25.4	22.0
13	herringbone wave	1.34	3	1.14	5.5	10.03	25.4	22.0
14	herringbone wave	1.49	3	1.14	5.5	10.03	25.4	22.0
15	herringbone wave	1.69	3	1.14	5.5	10.03	25.4	22.0
16	herringbone wave	1.81	4	1.14	5.5	10.03	25.4	22.0
17	herringbone wave	2.12	4	1.14	5.5	10.03	25.4	22.0
18	herringbone wave	2.54	4	1.14	5.5	10.03	25.4	22.0

tailed dimensions of the fin patterns are illustrated in Fig. 1. The waffle height of the herringbone wave fin was 1.14 mm. For all the heat exchanger samples, P_t was 25.0 mm, P_l was 22.0 mm, and D_c was 10.03 mm. The D_c was determined by measuring the tube outer diameter (including fin collar) from the samples. For the wave fin, the fin pitch was varied from 1.34 mm to 2.54 mm, and the number of tube rows was varied from one to four. For all the heat exchangers, smooth tubes were used at the tube-side, and the tubes were circuited to cross-counter configuration with single inlet and outlet.

2.2 Test apparatus and procedures

A schematic drawing of the apparatus is shown in Fig. 3. It consists of a suction-type wind tunnel, water circulation and control units, and a data acquisition system. The apparatus is situated in a constant temperature and humidity chamber. The airside inlet condition of the heat exchanger is maintained by controlling the chamber temperature and humidity. The inlet and outlet dry and wet bulb temperatures are measured by the sampling method suggested in ASHRAE Standard 41.1 [16]. A diffusion baffle is installed behind the test sample to mix the outlet air. The waterside inlet condition is maintained by regulating the flow rate and inlet temperature of the constant temperature bath situated outside of the chamber. Both the air and the water temperatures are measured by pre-calibrated RTDs (Pt-100 Ω sensors). Their

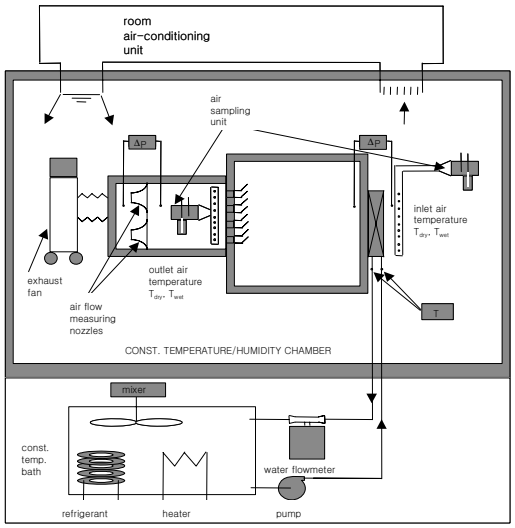

Fig. 3. Schematic drawing of the test setup.

accuracies are $\pm 0.1^{o}$C. The water flow rate is measured by a positive displacement type flow meter, whose accuracy is ± 0.0015 liter/s. The airside pressure drop across the heat exchanger is measured by using a differential pressure transducer. The air flow rate is measured by using a nozzle pressure difference according to ASHRAE Standard 41.2 [17]. The accuracy of the differential pressure transducers is ± 1.0 Pa.

During the experiment, the water temperature was held at 45^{o}C. The chamber temperature was maintained at 21^{o}C with 60% relative humidity. Experiments were conducted varying the frontal air velocity from 0.3 m/s to 3.5 m/s. The energy balance between the airside and the tube-side was within ± 3%. The discrepancy increased as the air velocity decreased. All the data signals were collected and converted by a data acquisition system (a hybrid recorder). The data were then transmitted to a personal computer for further manipulation. An uncertainty analysis was conducted following ASHRAE Standard 41.5 [18], and the results are listed in Table 3. The major uncertainty on the friction factor was the uncertainty of the differential pressure measurement (± 10%), and the major uncertainty on the heat transfer coefficient (or j factor) was that of the tube-side heat transfer coefficient (± 10%). The uncertainties decreased as the Reynolds number increased.

2.3 Data reduction

For the cross-counter configuration of the present study, appropriate equations for the heat exchanger analysis are given by Taborek [19]. The UA value is obtained from the following equations.

$$UA = (\dot{m}c_p)_{air} NTU_2 \tag{1}$$

$$NTU_2 = -2\ln(1-K) \tag{2}$$

The K is obtained from the following equations.

$$2 \text{ row}: \ \frac{K}{2} + (1-\frac{K}{2})\exp(2KR) = \frac{1}{1-RP} \tag{3}$$

Table 3. Uncertainty analysis.

Parameter	Max. Uncertainties
Temperature	± 0.1 K
Differential pressure	± 1.0 Pa
Water flow rate	± 1.5×10^{-6} m^3/s
Re_{Dc}	± 2%
f	± 10 %
j	± 12%

$$\text{3 row}: \begin{matrix} K[1-\frac{K}{4}-RK(1-\frac{K}{2})]\exp(KR) \\ +(1-\frac{K}{2})^2\exp(3KR)=\frac{1}{1-RP} \\ \frac{K}{2}(1-K+\frac{K^2}{4})+K(1-\frac{K}{2}) \end{matrix} \quad (4)$$

$$\text{4 row}: +[1-\frac{RK}{8}(1-\frac{K}{2})\exp(2KR)] \quad (5)$$
$$+(1-\frac{K}{2})^3\exp(4KR)=\frac{1}{1-RP}$$

$$R=\frac{T_{w,in}-T_{w,out}}{T_{air,out}-T_{air,in}} \quad (6)$$

$$P=\frac{T_{air,out}-T_{air,in}}{T_{w,in}-T_{air,in}} \quad (7)$$

For the one row configuration, a cross-flow $\varepsilon-NTU$ equation was used. The airside heat transfer coefficient is obtained from the following equation.

$$\frac{1}{\eta_o h_o A_o}=\frac{1}{UA}-\frac{1}{h_i A_i}-\frac{t}{k_t A_t} \quad (8)$$

The total surface area A_0 of the wave fins is an actual heat transfer area (not a projected area) that was used. The resulting A_0 of the sample having herringbone wave fins was 2.1% larger than those having plain fins. For the tube-side heat transfer coefficients, Gnielinski's Eq. [20] was used.

$$h_i=\frac{k_w}{D_i}\frac{(f_i/8)(\mathrm{Re}_{Di}-1000)\mathrm{Pr}_w}{1+12.7(f_i/8)^{1/2}(\mathrm{Pr}_w^{2/3}-1)} \quad (9)$$

$$f_i=(0.79\ln\mathrm{Re}_{Di}-1.64)^{-2} \quad (10)$$

For an accurate assessment of the airside heat transfer coefficient, it is important to minimize the tube-side thermal resistance. Throughout the experiment, the tube-side thermal resistance was less than 10% of the total thermal resistance.

The surface efficiency η_o is obtained from Eq. (11).

$$\eta_o=1-\frac{A_f}{A_o}(1-\eta) \quad (11)$$

The fin efficiency is given by Schmidt [21] as

$$\eta=\frac{\tanh(mr_c\phi)}{mr_c\phi} \quad (12)$$

where

$$m=\sqrt{\frac{2h_o}{k_f t_f}} \quad (13)$$

$$\phi=(\frac{R_{eq}}{r_c}-1)[1+0.35\ln(\frac{R_{eq}}{r_c})] \quad (14)$$

$$\frac{R_{eq}}{r_c}=1.28\frac{P_t}{r_c}(\frac{\sqrt{(P_t/2)^2+P_l^2}}{P_t}-0.2)^{0.5}: \mathrm{N}=1 \quad (15)$$

$$\frac{R_{eq}}{r_c}=1.27\frac{P_t}{r_c}(\frac{\sqrt{(P_t/2)^2+P_l^2}}{P_t}-0.3)^{0.5}: \mathrm{N}>1 \quad (16)$$

With Eqs. (8) to (16), an iterative procedure is needed to obtain the airside heat transfer coefficient h_o. In the figures, heat transfer coefficients are presented as j factors versus Re_{Dc}.

$$\mathrm{Re}_{Dc}=\frac{\rho_a V_{\max} D_c}{\mu_a} \quad (17)$$

$$j=\frac{h_o}{\rho_a V_{\max} c_{pa}}\mathrm{Pr}_a^{2/3} \quad (18)$$

All the fluid properties are evaluated at an average air temperature. The core friction factor is calculated from the measured pressure drop.

$$f=\frac{A_c}{A_o}\frac{\rho_m}{\rho_{in}}[\frac{2\Delta P\rho_{in}}{(\rho_m V_{\max})^2}-(1+\sigma^2)(\frac{\rho_{in}}{\rho_{out}}-1)] \quad (19)$$

In Eq. (19), the entrance and the exit loss coefficients are neglected following the suggestion by Wang et al. [22].

3. Results and discussions

To confirm the credibility of the present test, the present 2 row data are compared with those of Wang et al. [7], and the results are shown in Fig. 4. Both samples have approximately the same waffle height and fin pitch. Fig. 4 shows that the j and f factors are approximately the same, although Wang et al.'s sample shows slightly higher j and f factors. Slightly higher waffle height of Wang et al. may be responsible for the higher j and f factors. Generally, comparison of the fin-and-tube heat exchanger data with that from other sources is rather difficult due to the variation of fin surface geometries. Minimal differences may significantly affect the thermal performance. In addition, the fin-tube attachment depends on the manufacturing process, introducing additional thermal resistance, which is difficult to evaluate. The contact resistance is usually included in the airside heat transfer coefficient, which adds uncertainty on the comparison of the airside heat transfer coefficients.

Considering these factors, the agreement between the present data and those of Wang et al. shown in Figure 4 appears very good. Fig. 4 shows that the present j factors significantly deviate from those of Wang et al. at low Reynolds numbers. The present j factor curve shows a fall-off at low Reynolds numbers. The fall-off of the j factor curve at low Reynolds numbers has also been reported by Rich [23] and Wang et al. [24]. Wang et al. [24] argued that standing vortices, which formed behind the tubes at low Reynolds numbers, might be responsible for the decrease of the heat transfer coefficient. With the decrease of the tube diameter, the size of the standing vortices will also decrease, yielding less deterioration of the heat transfer coefficient. This might explain why Wang et al.'s [7] j factor curve does not fall-off at low Reynolds numbers. One other possible explanation could be that, at a small Reynolds numbers, NTU of the sample gets large and even a small uncertainty on the heat transfer measurement yields significant error on the j factor.

The effect of fin pitch on j and f factors is shown in Fig. 5 for different tube rows. For one or two row samples, the fin pitch was varied from 1.34 mm to 2.54 mm. For three row samples, the fin pitch was varied from 1.34 mm to 1.69 mm, and it was varied

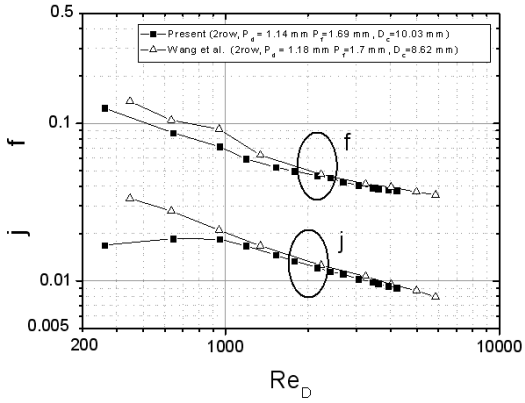

Fig. 4. The present two row data compared with those of Wang et al. [7].

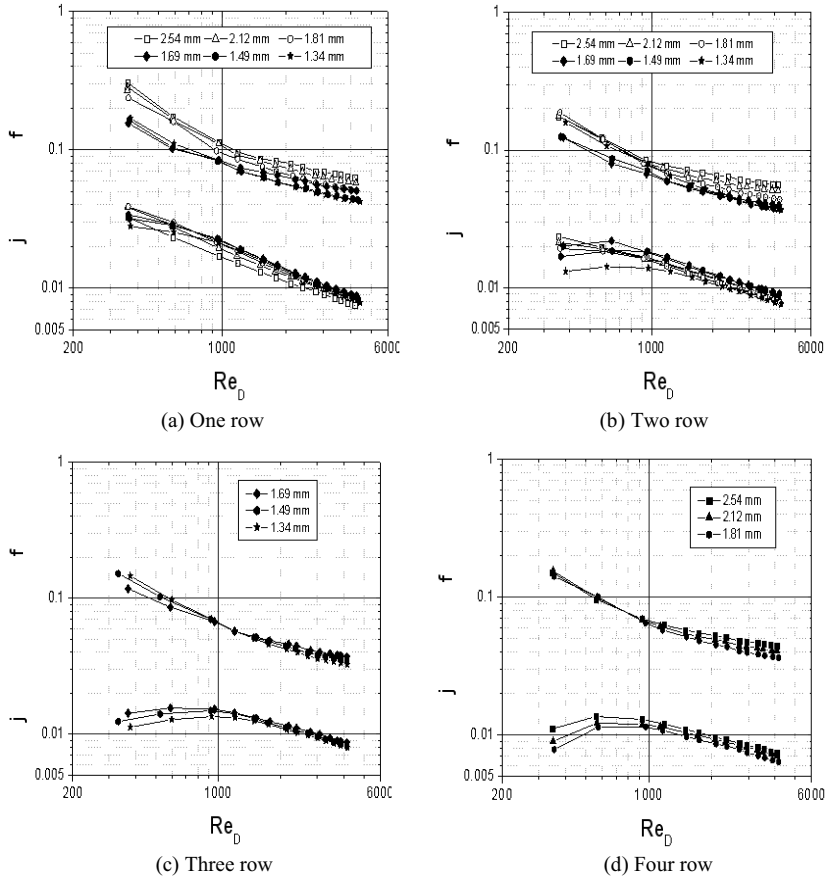

(a) One row (b) Two row

(c) Three row (d) Four row

Fig. 5. Effect of fin pitch on the j and f factors for different tube rows.

from 1.81 mm to 2.54 mm for four row samples. Figure 5 shows that the effect of fin pitch on j factor is not significant, although a slight decrease of j factor for increased fin pitch is noticed for one row samples. The independence of j factor on fin pitch has also been noticed by many investigators for wavy fin configurations [7, 8, 10] and for a plain fin configuration [23]. Different from the j factor, the f factor increases as the fin pitch increases. As the row number increases, however, the effect of fin pitch on f factor gets less significant. The increase of f factor with the fin pitch has also been reported by many researchers [7-11, 23]. Torikoshi et al. [25] performed a three-dimensional unsteady numerical computation for one row plate fin-and-tube heat exchangers having various fin pitches (from 1.7 mm to 3.0 mm for D_c = 10 mm). They reported that the downstream flow pattern was strongly affected by the fin pitch. As the fin pitch increased, the downstream flow field became more unsteady, which apparently increased the pressure drop of the heat exchanger. However, the flow field in the region between the fins remained steady even at the largest fin pitch. The heat transfer on the fin surface was also unaffected by the fin pitch, which yielded fin-pitch-independent j factors. Although the numerical study is limited to a plain fin configuration, similar arguments may apply to a wavy fin configuration, especially to samples having small waffle height such as those used in the present study.

The effect of tube row on the j and f factor is shown in Fig. 6 for three different fin pitches (P_f = 2.54, 1.69, 1.34 mm). These figures show that both j and f factors are significantly influenced by the number of tube rows. The j factors decrease as the number of tube rows increases. However, as the Reynolds number increases, the effect of tube row diminishes. For fin-and-tube heat exchangers, air flows through channels formed by narrow-spaced fins and intermediate tubes. For a channel flow, the heat transfer is the largest at the inlet of the channel, and decreases downstream. Thus, we may expect a larger j factor for samples having smaller number of rows (having short channels). However, at a sufficiently large Reynolds number, the turbulence generated by the tubes governs the heat transfer process, and the effect of tube row diminishes. Rich [26], Wang et al. [7], Wang et al. [9] report the same trend for the j factor. Fig. 6 shows that the f factor also decreases as the number of tube row increases. Same arguments as those provided for the j factor may apply to the f factor. Jang and Chen [27], Min et al. [28] reported the same trend for the f factor. However, minimal dependency of the f factor on the number of tube row was reported by Wang et al. [7, 8]. Fig. 6 shows that the f factor dependency on the tube row decreases as the fin pitch decreases.

The literature reveals two heat transfer and pressure drop correlations [5, 29] applicable to herringbone

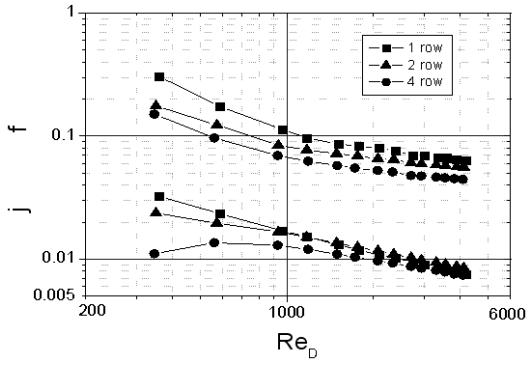

(a) P_f = 2.54 mm

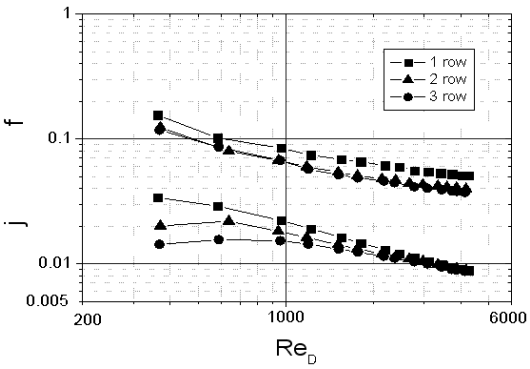

(b) P_f = 1.69 mm

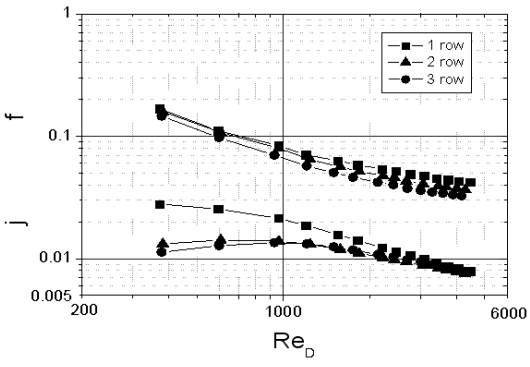

(c) P_f = 1.34 mm

Fig. 6. Effect of tube row on the j and f factors for different fin pitches.

wave fin-and-tube heat exchangers. Kim et al. [5] developed a correlation based on 41 wave fin geometries of Beecher and Fagan [6] and Wang et al. [7]. Wang et al. [29] developed a correlation based on their own data [7-10]. The present j and f factors are compared with the predictions in Fig. 7. Figs. 7(a) and 7(b) show that both correlations highly overpredict the present j factors. The overprediction increases as the number of tube row increases. The standard deviation of the predictions by Kim et al. [5] correlation is 55.9 %, and that by Wang et al. [29] correlation is 67.6 %. The standard deviation is defined as

$$SD = \sqrt{\frac{\sum (j_{pred}/j_{exp} - 1)^2}{N}} \tag{18}$$

In Figs. 7(c) and 7(d), the present f factors are compared with the correlations. The Kim et al. [5] correlation reasonably predicts the friction data except for the one row f factors. The one row data are highly underpredicted. Wang et al.'s [29] correlation generally overpredicts the present data. The standard deviation of the predictions by Kim et al. correlation is 19.6 %, and that by Wang et al. correlation is 29.2 %. As shown in Table 1, the waffle height and the corrugation angle of present samples are 1.14 mm and 11.7°, which are the smallest values ever tested. The overprediction of the present data by the correlations may be due to the small waffle height of the present samples.

Due to the failure of existing correlations to adequately predict the present data, an attempt was made to develop a new correlation. A new correlation was developed extending the Kim et al. [5] correlation by adding Wang et al. [8, 9] and the present data to those of Wang et al. [7]. Beecher and Fagan [6] data, which were included in the Kim et al. [5] correlation, were excluded because Beecher and Fagan's samples do not adequately simulate a practical heat exchanger. Their models consisted of a pair of brass plates and spacers to simulate a fin-and-tube geometry, and the channel walls were electrically heated. Therefore, the

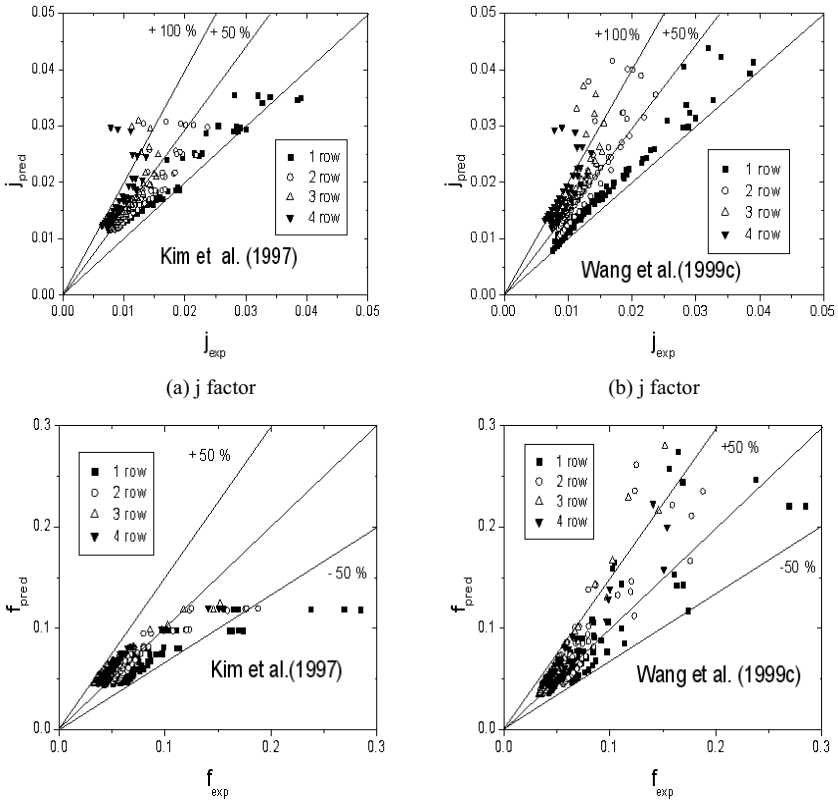

(a) j factor (b) j factor

(c) f factor (d) f factor

Fig. 7. Present data compared with the predictions by existing correlations.

contact resistance between fin and tube, which is inherent in an actual heat exchanger, does not appear in Beecher and Fagan's data. The contact resistances are generally included in the airside heat transfer coefficient.

A multiple regression technique was carried out to correlate the data. The potentially significant variables are: flow variables (Re_{Dc}), tube bank geometric variables (D_c, P_t, P_l, N and tube layout), and fin geometry variables (s, x_f, P_d, etc.). Several different groupings of the dimensionless variables were tried in the development of the correlation. The set finally chosen was based on the groupings that provided the best correlation. The resulting correlation is given by

$$j_3 = 0.170\,\mathrm{Re}^{-0.339}\left(\frac{P_t}{P_l}\right)^{0.193}\left(\frac{s}{D_c}\right)^{-1.83}\left(\frac{x_f}{P_d}\right)^{-2.75}\left(\frac{P_d}{s}\right)^{-1.84} \quad (\mathrm{N}\geq 3) \tag{19}$$

$$j_N = (1.69 - 0.254N)\, j_3 \quad (\mathrm{Re_{Dc}} \leq 1000,\ \mathrm{N} = 1, 2) \tag{20}$$

$$j_N = (1.04 + 0.0067N)\, j_3 \quad (\mathrm{Re_{Dc}} > 1000,\ \mathrm{N} = 1, 2) \tag{21}$$

$$f = f_f \frac{A_f}{A} + f_t\left(1 - \frac{A_f}{A}\right)\left(1 - \frac{t_f}{P_f}\right) \tag{22}$$

$$f_f = 2.061\,\mathrm{Re}^{-0.511}\left(\frac{P_t}{P_l}\right)^{0.754}\left(\frac{s}{D_c}\right)^{-0.241}\left(\frac{x_f}{P_d}\right)^{-0.221}\left(\frac{P_d}{s}\right)^{-0.113} N^{-0.0664} \tag{23}$$

$$f_t = \frac{1}{\pi}\left[0.25 + \frac{0.118}{(P_t/D_c - 1)^{1.08}\,\mathrm{Re}_{Dc}^{\,0.16}}\right]\left(\frac{P_t}{D_c} - 1\right) \tag{24}$$

In Eqs. (19) to (21), j_3 implies j factor of the heat exchanger having more than three rows. For one or two-row configuration, Eqs. (20) and (21) are used to predict the j factor depending on the Reynolds number. The friction factor is obtained from Eq. (22), which consists of the friction by the fin (Eq. 23) and that by the tube (Eq. 24). Equation (24) was proposed by Jakob [30] to predict the friction factor of a staggered tube bundle. Equation (23) was obtained by multiple regression of the data.

The new correlation is compared with the data in Fig. 8. The standard deviation is 15.4% for the friction factor and 38.8% for the j factor. When the present data (shown as dark symbols in the figure) are compared with the correlation, the standard deviation of the f factors is 16.7%, and that of the j factors is 20.8%, which are significant improvements over Kim et al. [5] or Wang et al. [29] correlation. The applicable range of the new correlation is

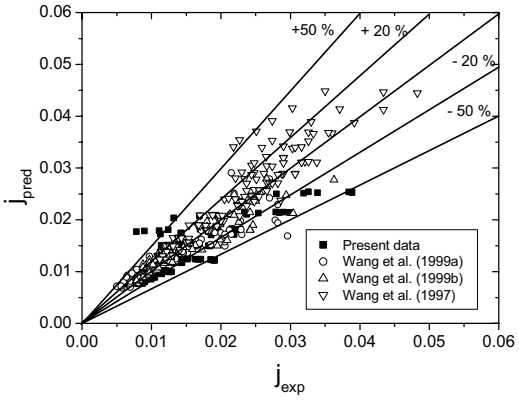

(a) j factor

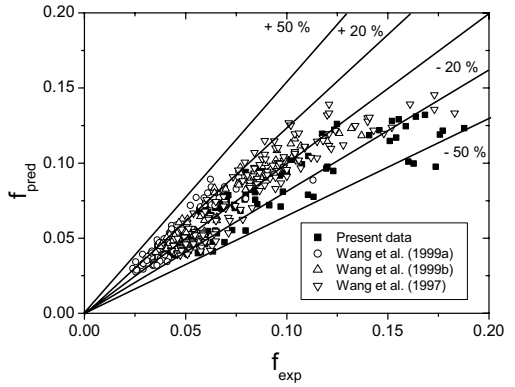

(b) f factor

Fig. 8. Comparison of j and f factors with the predictions by the new correlation.

$1.15 \leq P_t/P_l \leq 1.33,\ 0.13 \leq s/D_c \leq 0.44,\ 3.01 \leq x_f/P_d \leq 4.82,$
$0.30 \leq P_d/s \leq 1.03$

4. Conclusions

In this study, the heat transfer and friction characteristics of heat exchangers having herringbone wave fins were experimentally investigated. Eighteen samples which had different fin pitches (1.34 mm to 2.54 mm) and tube rows (one to four) were tested. The waffle depth was 1.14 mm, and the corrugation angle was 11.7°. Data are compared with existing correlations. Listed below are major findings.

(1) The j factors are insensitive to the fin pitch, while f factors increase as the fin pitch increases.
(2) Both the j and f factors decrease as the number of tube rows increases. However, as the Reynolds number increases, the effect of tube row diminishes, at least for j factors.
(3) Existing correlations fail to adequately predict the

present data. A new correlation was developed based on the existing data, which significantly improves the predictions of the present data (standard deviation of the f factors 16.7 % and that of the j factors 20.8%).

Nomenclature

A : Heat transfer area (m^2)
A_c : Minimum free flow area (m^2)
A_t : Heat transfer area at the mid-plane of the tube wall (m^2)
c_p : Specific heat (J $kg^{-1}s^{-1}$)
D_c : Tube diameter including fin collar thickness (m)
D_i : Tube-side diameter (m)
D_r : Maximum tube-side diameter (to the fin root) (m)
f : Friction factor, see Eq. (19) (dimensionless)
f_i : Tube-side friction factor, see Eq. (10) (dimensionless)
G : Mass flux (kg m^{-2})
h : Heat transfer coefficient (W m^{-2} K^{-1})
j : Colburn j factor, $\frac{h_\sigma}{\rho_a V_{\max} c_{pa}} \mathrm{Pr}_a^{2/3}$ (dimensionless)
k_t : Thermal conductivity of the tube (W m^{-1} K^{-1})
k_w : Thermal conductivity of water (W m^{-1} K^{-1})
N : Number of tube row or number of data (dimensionless)
NTU : Number of transfer units, see Eq. (2) (dimensionless)
P_d : Fin pattern depth, peak to valley excluding fin thickness (m)
P_f : Fin pitch (m)
P_t : Transverse tube pitch (m)
P_l : Longitudinal tube pitch (m)
Pr : Prandtl number (dimensionless)
r_c : Tube radius including fin collar (m)
R_{eq} : Equivalent radius (m)
$\mathrm{Re_{Dc}}$: Reynolds number based on D_c, $\frac{\rho_a V_{\max} D_c}{\mu_a}$ (dimensionless)
$\mathrm{Re_{Di}}$: Tube-side Reynolds number (dimensionless)
s : Fin spacing (m)
t : Tube wall thickness (m)
T : Temperature (K)
t_f : Fin thickness (m)
U : Overall heat transfer coefficient (W m^{-2} s^{-1})
V_{max} : Maximum airside velocity (m s^{-1})
x_f : Projected fin pattern length for one-half wave length (m)

Greek letters

ΔP : Pressure loss (Pa)
η : Fin efficiency, see Eq. (12) (dimensionless)
η_o : Surface efficiency, see Eq. (11) (dimensionless)
ρ : Density (kg m^{-3})
μ : Dynamic viscosity (kg m^{-1} s^{-1})
σ : Contraction ratio of the cross-sectional area (dimensionless)

Subscripts

2 : Subscript of NTU, see Eq. (2)
a : Air
c : Fin collar
exp : Experimental
i : Tube-side
in : Inlet
f : Fin
m : Mean
o : Airside
out : Outlet
pred : Prediction
t : Tube wall
w : Water

References

[1] R. L. Webb and N. H. Kim, Principles of enhanced heat transfer, Taylor and Francis Pub. (2005).
[2] C. C. Wang, On the Airside Performance of Fin-and-Tube Heat Exchangers, in S. Kakac et al. (Eds.) Heat Transfer Enhancement of Heat Exchangers. Kluwer Academic Press, (1999) 141-162.
[3] L. Goldstein and E. M. Sparrow, Experiments on the Transfer Characteristics of a Corrugated Fin-and-Tube Heat Exchanger Configuration, *J. Heat Transfer* 98 (1976) 26-34.
[4] M. M. Ali and S. Ramadhyani, S., Experiments on Convective Heat Transfer in Corrugated Channels, *Experimental Heat Transfer* 5 (1992) 175-193.
[5] N.-H. Kim, J.-H. Yun and R. L. Webb, Heat Transfer and Friction Correlations for Wavy Plate Fin-and-Tube Heat Exchangers, *J. Heat Transfer* 119 (1997) 560-567.
[6] D. T. Beecher and T. J. Fagan, Effects of Fin Pattern on the Airside Heat Transfer Coefficients in

Plate Finned Tube Heat Exchangers, *ASHRAE Trans.* 93 (2) (1987) 1961-1984.

[7] C. C. Wang, W. L. Fu and C. T. Chang, Heat Transfer and Friction Characteristics of Typical Wavy Fin-and-Tube Heat Exchangers, *Exp. Thermal Fluid Science* 14 (1997) 174-186.

[8] C. C. Wang, Y. M. Tsai and D. C. Lu, Comprehensive Study of Convex Louver and Wavy Fin-and-Tube Heat Exchangers, *J. Thermophysics Heat Transfer* 12 (3) (1998) 423-430.

[9] C. C. Wang, Y. T. Lin, C. J. Lee and Y. J. Chang, Investigation of Wavy Fin-and-Tube Heat Exchangers: A Contribution to Databank, *Experimental Heat Transfer* 12 (1999) 73-89.

[10] C. C. Wang, Y. J. Chang and N. F. Chiou, Effects of Waffle Height on the Airside Performance of Wavy Fin-and-Tube Heat Exchangers, *Heat Transfer Engineering* 20 (3) (1999) 45-56.

[11] J. M. Saiz Jabardo, J. R. Bastos Zoghbi Filho and A. Salamanca, Experimental Study of the Airside Performance of Louver and Wave Fin-and-Tube Coils, *Exp. Thermal Fluid Science* 30 (2006) 621-631.

[12] S. Wongwises and Y. Chokeman, Effect of Fin Thickness on Airside Performance of Herringbone Wavy Fin-and-Tube Heat Exchangers, *Heat Mass Transfer* 41 (2004) 147-154.

[13] Y. Chokeman and S. Wongwises, Effect of Fin Pattern on the Airside Performance of Herringbone Wavy Fin-and-Tube Heat Exchangers, *Heat Mass Transfer* 41 (2005) 642-650.

[14] D. R. Mirth and S. Ramadhyani, Correlations for Predicting the Airside Nusselt Numbers and Friction Factors in Chilled Water Cooling Coils, *Experimental Heat Transfer* 7 (1994) 143-162.

[15] N.-H. Kim, J.-P. Cho and Y. Baek, An Experimental Investigation on the Airside Performance of Fin-and-Tube Heat Exchangers Having Sinusoidal Wave Fins, *Korean J. Air-Conditioning and Refrigeration* 16 (4) (2004) 355-367.

[16] ASHRAE Standard 41.1, Standard Method for Temperature Measurement (1986).

[17] ASHRAE Standard 41.2, Standard Method for Laboratory Air-Flow Measurement (1987).

[18] ASHRAE Standard 41.5, Standard Measurement Guide, Engineering Analysis of Experimental Data (1975).

[19] J. Taborek, F and θ Charts for Cross-Flow Arrangements, in: G. F. Hewitt (Ed.) *Heat Exchanger Design Handbook*. Section 1.5.3, Begell House Inc. (1998).

[20] V. Gnielinski, New Equation for Heat and Mass Transfer in Turbulent Pipe and Channel Flow, *Int. Chem. Eng*. 16 (1976) 359-368.

[21] T. E. Schmidt, Heat Transfer Calculations for Extended Surfaces, *J of ASRE, Refrigeration Engineering* 4 (1949) 351-357.

[22] C. C. Wang, R. L. Webb and K. Y. Chi, Data Reduction for Airside Performance of Fin-and-Tube Heat Exchangers, *Experimental Thermal Fluid Science* 21 (2000) 218-226.

[23] D. G. Rich, The Effect of Fin Spacing on the Heat Transfer and Friction Performance of Multi-Row, Plate Fin-and-Tube Heat Exchangers, *ASHRAE Trans*. 79 (2) (1973) 137-145.

[24] C. C. Wang, Y. J. Chang, Y. C. Hsieh and Y. T. Lin, Y. T., Sensible Heat and Friction Characteristics of Plate Fin-and-Tube Heat Exchangers Having Plain Fins, *Int. J. Refrigeration* 19 (4) (1996) 223-230.

[25] D. G. Rich, The Effect of the Number of Tube Rows on Heat Transfer Performance of Smooth Plate Fin-and-Tube Heat Exchangers, *ASHRAE Trans*. 81 (1) (1975) 307-317.

[26] K. Torikoshi, G. N. Xi., Y. Nakazawa and H. Asano, Flow and Heat Transfer Performance of a Plate Fin and Tube Heat Exchanger (First Report: Effect of Fin Pitch), Heat Transfer 1994, Proceedings of the 10th Int. Heat Transfer Conf., 4 (1994) 411-416.

[27] J.-Y. Jang and L.-K. Chen, Numerical Analysis of Heat Transfer and Fluid Flow in a Three-Dimensional Wavy Fin-and-Tube Heat Exchanger, *Int. J. Heat Mass Transfer* 40 (16) (1997) 3981-3990.

[28] C.-K. Min, J.-P. Cho, W.-K. Oh and N.-H. Kim, Heat Transfer and Pressure Drop Characteristics of Heat Exchangers Having Plain Fins Under Dry and Wet Conditions, *Korean J. Air-Conditioning and Refrigeration* 16 (3) (2004) 218-229.

[29] C. C. Wang, J. Y. Jang and N. F. Chiou A Heat Transfer and Friction Correlation for Wavy Fin-and-Tube Heat Exchangers, *Int. J. Heat Mass Trans*., 42 (1999) 1919-1924.

[30] M. Jakob, Heat Transfer and Flow Resistance in Crossflow of Gases over Tube Banks, Trans. ASME 60 (1938) 384.